

Geometric determination of the hyperbolic paraboloids of the vaults in the entrance porch to the Crypt of Colònia Güell by Antoni Gaudí

Determinación geométrica de los paraboloides hiperbólicos de las bóvedas que configuran el pórtico de acceso a la Cripta de la Colonia Güell de Antoni Gaudí

A. Cortés (*), A. Samper (*), B. Herrera (*)

ABSTRACT

The Crypt of Colonia Güell (1898-1914), designed by the architect Antoni Gaudí, is an asset of cultural interest and historical heritage of Spain. According to some historians and architects, the first vaults with the form of a hyperbolic paraboloid that have been described are found on the roof of the entrance porch to the Crypt. The present study aims to verify the previous statement using an objective geometric method. With this process we determine: 1) What are the 19 hyperbolic paraboloids that best fit the surfaces generated by the 19 fragments of vaults at the entrance porch; 2) We offer an objective measure of this fit and, 3) We classify those paraboloids based on their geometric parameters.

Keywords: Architectural surface, geometric determination, Colonia Güell, hyperbolic paraboloid, Antoni Gaudí.

RESUMEN

La Cripta de la Colonia Güell (1898-1914) diseñada por el arquitecto Antoni Gaudí, es un bien de interés cultural y patrimonio histórico de España. Según algunos historiadores y arquitectos, las primeras bóvedas de la historia de la arquitectura con forma de paraboloides hiperbólicos se encuentran en el techo del pórtico de acceso a la cripta. El presente estudio pretende comprobar la anterior afirmación con un método geométrico objetivo. Con este proceso determinamos: 1) Cuáles son los 19 paraboloides hiperbólicos que mejor se ajustan a las superficies generadas por los 19 fragmentos de bóvedas que conforman el pórtico; 2) Ofrecemos una medida objetiva de tal ajuste y, 3) Presentamos una clasificación de tales paraboloides mediante sus parámetros geométricos.

Palabras clave: Superficie arquitectónica, Determinación geométrica, Colonia Güell, paraboloides hiperbólicos, Antoni Gaudí.

(*) Universitat Rovira i Virgili (España).

Persona de contacto/Corresponding author: blas.herrera@urv.cat (B. Herrera)

ORCID: <https://orcid.org/0000-0001-9116-7647> (A. Cortés); <https://orcid.org/0000-0002-4795-2127> (A. Samper), <https://orcid.org/0000-0003-2924-9195> (B. Herrera)

Cómo citar este artículo/Citation: Cortés, A.; Samper, A.; Herrera, B. (2019). Geometric determination of the hyperbolic paraboloids of the vaults in the entrance porch to the Crypt of Colònia Güell by Antoni Gaudí. *Informes de la Construcción*, 71(554): e295. <https://doi.org/10.3989/ic.63691>

Copyright: © 2019 CSIC. This is an open-access article distributed under the terms of the Creative Commons Attribution 4.0 International (CC BY 4.0).

Recibido/Received: 04/03/2018
Aceptado/Accepted: 27/06/2018
Publicado on-line/Published on-line: 11/07/2019

1. INTRODUCTION

The Colònia Güell was a purpose-built industrial district in Santa Coloma de Cervelló (Barcelona). Its construction began in 1890 on the initiative of Eusebi Güell y Bacigalupi, a Spanish entrepreneur. The crypt of the church, commissioned by Güell and designed by Antoni Gaudí (1-2), is the most remarkable building in this complex. Despite remaining unfinished following the death of its owner in 1918, the crypt has been the subject of many studies because of its structural and geometric innovation. According to (1), hyperbolic paraboloids were used here for the first time in the history of architecture. For this reason, and also because of the architectural prowess of the indoor space and the entrance porch, this building is considered to be one of the key pieces of the twentieth century architecture.

The porch giving access to the crypt comprises a set of pillars, arches and vaults. These vaults fill the triangular and trapezoidal voids of the arch structure (Figure 1). According to (1, 3), the normal solution would have been to build positive double-curvature vaults, which were very common amongst the Catalan architects at the time (4-5). Despite that, (6) claims that these are the first vaults in the history of architecture having the shape of a hyperbolic paraboloid.

When talking about the architectural composition and morphology of the entrance porch, it is claimed that all of its 19 vaults were designed in the shape of hyperbolic paraboloids – in this regard, readers may turn to the following bibliographic references: (1, 2, 3, 6, 7, 8, 9, 10, 11). Besides, 13 of these surfaces are decorated with coloured ceramic crosses which, according to (1), follow the straight directrices of these hyperbolic paraboloids (Figures 3-4).

This purpose of this paper is to check if those claims are true.

In order to achieve our results, we use a mathematically objective method to find the 19 hyperbolic paraboloids which best fit the surfaces of the 19 vaults forming the entrance porch to the crypt of Colònia Güell (Figures 2 and 3), and we also provide an objective measurement of that fit.

This method does not involve mechanical, constructive or structural processes; it only involves standard geometric processes, numerical processes, computing, statistics and 3D data acquisition. Lastly, using these techniques we provide the geometric parameters of these paraboloids.

Figures 2 and 3 below show the aforementioned 19 vaults in their entirety. For this reconstruction, we have used photogrammetrical techniques and 3D modelling with commercial software PhotoScan and MeshLab.

2. METHOD USED TO DETERMINE THE HYPERBOLIC PARABOLOID AND ITS GEOMETRIC ELEMENTS

2.1. Geometric regression

Let $\mathcal{N} = \{P_i\}_{i=1}^{i=n}$ be the point cloud outlining the surface contour of a vault in the entrance porch to the crypt of Colònia Güell. These points were obtained using photogrammetrical techniques and the software PhotoScan. Table 1 shows the number n of points in each of the clouds forming the studied vaults. For these points, we use 3D coordinates (x', y', z') according to the 3D orthonormal coordinate system $\mathcal{R}' = \{O; \vec{u}_1, \vec{u}_2, \vec{u}_3\}$ of the scanning device (Figures 4 and 5).



Figure 1. Entrance porch to the crypt of Colònia Güell by Antoni Gaudí. [Picture taken by the authors.]



Figure 2. Three-dimensional model of the 19 vaults forming the entrance porch to the crypt. [Image generated by the authors].



Figure 3. Orthogonal projection on the ground plane of the 19 vaults forming the entrance porch to the crypt. In the right image, the 13 vaults which bear a coloured ceramic cross on their surfaces are highlighted in red. The triangle pinpoints the location of the entrance to the crypt. [Image generated by the authors].

It is to be noted that the spatial position of this reference \mathcal{R} is geometrically unknown at the start of calculations.

The geometric determination process begins by changing from the initial coordinates to the coordinates $(x, y, z)_{\varphi\theta\alpha}$ of the following orthonormal reference system $\mathcal{R}_{\varphi\theta\alpha} = \{O; \vec{e}_{1\varphi\theta\alpha}, \vec{e}_{2\varphi\theta\alpha}, \vec{e}_{3\varphi\theta\alpha}\}$ which is mobile depending on φ , θ and α , as follows [1-2-3-4-5-6]:

$$\vec{v}_{1\varphi\theta} = \sin\left(\varphi + \frac{\pi}{2}\right)\cos(\theta)\vec{u}_1 + \sin\left(\varphi + \frac{\pi}{2}\right)\sin(\theta)\vec{u}_2 + \cos\left(\varphi + \frac{\pi}{2}\right)\vec{u}_3 \quad [1]$$

$$\vec{v}_{2\varphi\theta} = -\sin(\theta)\vec{u}_1 + \cos(\theta)\vec{u}_2 \quad [2]$$

$$\vec{v}_{3\varphi\theta} = \sin(\varphi)\cos(\theta)\vec{u}_1 + \sin(\varphi)\sin(\theta)\vec{u}_2 + \cos(\varphi)\vec{u}_3 \quad [3]$$

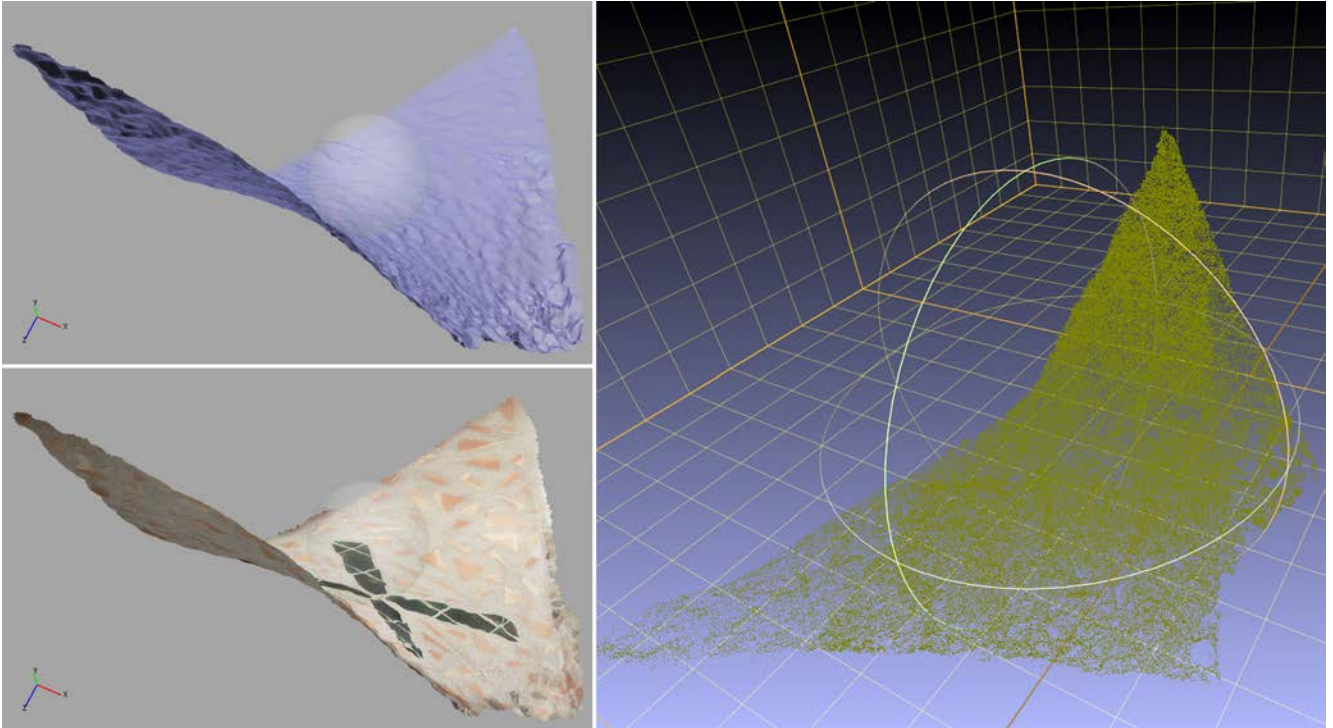


Figure 4. Three-dimensional model of vault number 5, as generated with the software PhotoScan; its cloud \mathcal{N} is made up by $n = 148622$ points. [Image generated by the authors.]

Table 1. Number n of points in each of the clouds \mathcal{N} forming the studied vaults.

Vault #	Number of points n in cloud \mathcal{N}	Vault #	Number of points n in cloud \mathcal{N}
1	50046	11	415198
2	125451	12	371637
3	125645	13	98293
4	179999	14	350632
5	148622	15	212260
6	31180	16	245032
7	320018	17	364235
8	380264	18	293295
9	438630	19	228404
10	281882	-	-

where $\varphi \in [0, \pi)$, $\theta \in [0, \pi)$.

$$\vec{e}_{1\varphi\theta\alpha} = \cos(\alpha)\vec{v}_{1\varphi\theta} + \sin(\alpha)\vec{v}_{2\varphi\theta} \quad [4]$$

$$\vec{e}_{2\varphi\theta\alpha} = -\sin(\alpha)\vec{v}_{1\varphi\theta} + \cos(\alpha)\vec{v}_{2\varphi\theta} \quad [5]$$

$$\vec{e}_{3\varphi\theta\alpha} = \vec{v}_{3\varphi\theta} \quad [6]$$

where $\alpha \in [0, \pi)$.

We said that the orthonormal reference system $\mathcal{R}_{\varphi\theta\alpha}$ is mobile depending on φ , θ and α because $\mathcal{R}_{\varphi\theta\alpha}$ is the rotation of system $\mathcal{R}' = \{O; \vec{u}_1, \vec{u}_2, \vec{u}_3\}$ when φ , θ and α change. A progressive way of generating that rotation is as follows: First (using formula [3] and angular amplitudes φ , θ), we place a unit vector $\vec{v}_{3\varphi\theta}$ in any position. Second (using formula [2] and angular amplitude θ), we place unit vector $\vec{v}_{2\varphi\theta}$ in such a way that it is

perpendicular to $\vec{v}_{3\varphi\theta}$ and lies within linear subspace $\langle \vec{u}_1, \vec{u}_2 \rangle$. Third (using formula [1]), by means of cross product we generate vector $\vec{v}_{1\varphi\theta}$ such that the basis $\{\vec{v}_{1\varphi\theta}, \vec{v}_{2\varphi\theta}, \vec{v}_{3\varphi\theta}\}$ is orthonormal and direct. Fourth (using formulas [4-5] and angular amplitude α), we rotate vectors $\{\vec{v}_{1\varphi\theta}, \vec{v}_{2\varphi\theta}\}$ around vector $\vec{v}_{3\varphi\theta} = \vec{e}_{3\varphi\theta\alpha}$ (formula [6]), thus obtaining the rotated vectors $\{\vec{e}_{1\varphi\theta\alpha}, \vec{e}_{2\varphi\theta\alpha}\}$ such that the basis $\{\vec{e}_{1\varphi\theta\alpha}, \vec{e}_{2\varphi\theta\alpha}, \vec{e}_{3\varphi\theta\alpha}\}$ is orthonormal and direct.

Therefore, after defining parameters φ , θ and α , we have the coordinates $(x_i, y_i, z_i)_{\varphi\theta\alpha}$ in the reference system $\mathcal{R}_{\varphi\theta\alpha}$ for each of the points P_i in the cloud $\mathcal{N} = \{P_i\}_{i=1}^{i=n}$.

Next we calculate $\Gamma_{\varphi\theta\alpha}$, which is the surface of the regression hyperbolic paraboloid which fits to cloud \mathcal{N} , and we obtain the following equation Eq. [7] in the reference system $\mathcal{R}_{\varphi\theta\alpha}$:

$$\Gamma_{\varphi\theta\alpha} \equiv 0 = B_{\varphi\theta\alpha}x^2 + C_{\varphi\theta\alpha}y^2 + H_{\varphi\theta\alpha}x + I_{\varphi\theta\alpha}y + J_{\varphi\theta\alpha}z + 1 \quad [7]$$

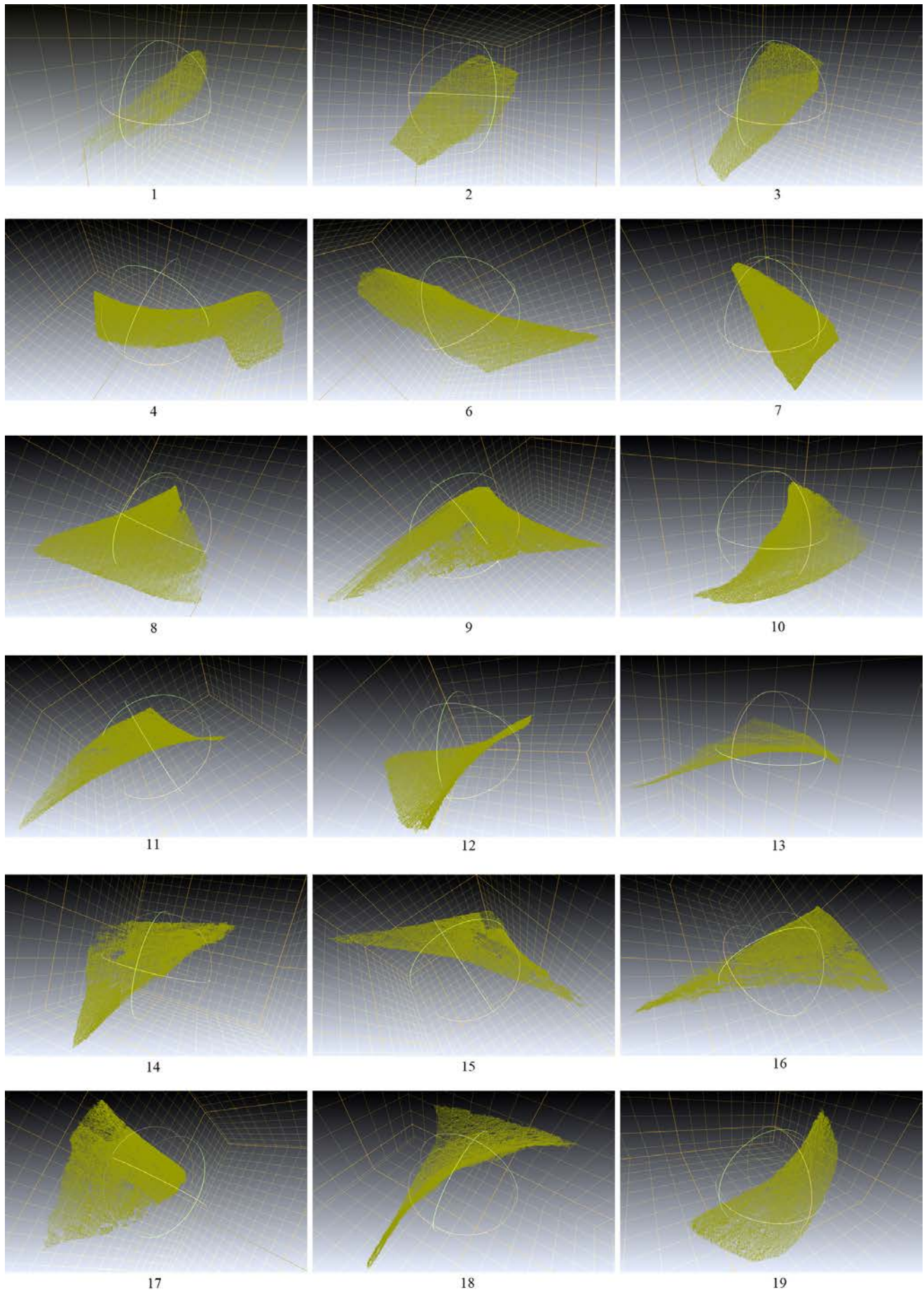


Figure 5. Three-dimensional renderings of the point clouds \mathcal{N} which define the studied vaults (except for cloud 5, which is displayed in more detail in Figure 4 above). [Image generated by the authors.]

This regression surface, $\Gamma_{\varphi\theta\alpha}$, described by Eq. [7] in the reference system $\mathcal{R}_{\varphi\theta\alpha}$, is the one which best fits the point cloud $\mathcal{N} = \{P_i\}_{i=1}^{i=n}$, minimizing the sum of the quadratic residues $\sum_{i=1}^{i=n} \varepsilon_i^2 = \sum_{i=1}^{i=n} (Bx_i^2 + Cy_i^2 + Hx_i + Iy_i + Jz_i + 1)^2$, being $B_{\varphi\theta\alpha} C_{\varphi\theta\alpha} < 0$. Eqs. [8] below are the Gauss normal equations which provide the solution to the calculation problem of $\Gamma_{\varphi\theta\alpha}$. This equations have a range of variation 1–n in Einstein summation convention, being $1_i = 1$. For example, $x_i^2 y_i = \sum_{i=1}^{i=n} x_i^2 y_i$, and $1_i x_i^3 = \sum_{i=1}^{i=n} x_i^3$.

$$\begin{pmatrix} 1_i x_i^4 & x_i^2 y_i^2 & 1_i x_i^3 & x_i^2 y_i & x_i^2 z_i \\ x_i^2 y_i^2 & 1_i y_i^4 & y_i^2 x_i & 1_i y_i^3 & y_i^2 z_i \\ 1_i x_i^3 & y_i^2 x_i & 1_i x_i^2 & x_i y_i & x_i z_i \\ x_i^2 y_i & 1_i y_i^3 & x_i y_i & 1_i y_i^2 & y_i z_i \\ x_i^2 z_i & y_i^2 z_i & x_i z_i & y_i z_i & 1_i z_i^2 \end{pmatrix} \begin{pmatrix} B \\ C \\ H \\ I \\ J \end{pmatrix} = \begin{pmatrix} -1_i x_i^2 \\ -1_i y_i^2 \\ -1_i x_i \\ -1_i y_i \\ -1_i z_i \end{pmatrix} \quad [8]$$

Remark: Formula [7] is the reason why we rotate the system \mathcal{R}' when φ , θ and α change, thus obtaining the system $\mathcal{R}_{\varphi\theta\alpha}$. It is not true that the equation of any hyperbolic paraboloid in system \mathcal{R}' takes the form $0 = Bx'^2 + Cy'^2 + Hx' + Iy' + Jz' + 1$. Actually, the equation of the hyperbolic paraboloid Γ_δ which best fits the cloud \mathcal{N} generated by the vault in system \mathcal{R}' takes the form $0 = Bx'^2 + Cy'^2 + Dz'^2 + Ex'y' + Fx'z' + Gy'z' + Hx' + Iy' + Jz' + 1$, where $0 = -CF^2 + FGE - BG^2 - DE^2 + 4BCD$ and where $0 < F^2I^2 - 4CF^2 - 2FGHI + 4FGE + 4CFHJ - 2FJEI + G^2H^2 - 4BG^2 - 2GHJE + 4BGJI - 4CDH^2 + 4DHEI + J^2E^2 - 4BCJ^2 - 4DE^2 - 4BDI^2 + 16BCD$. Nonetheless, what matters here is not the equation for Γ_δ , but the paraboloid Γ_δ itself. Therefore, instead of finding Γ_δ in the system \mathcal{R}' , we do as follows: First, we find the hyperbolic paraboloid $\Gamma_{\varphi\theta\alpha}$ which fits cloud \mathcal{N} such that the equation of this hyperbolic paraboloid in the system $\mathcal{R}_{\varphi\theta\alpha}$ takes the form [7]; and then, as we will see in sections 2.2 and 2.3, we vary the angle distances φ , θ and α until we find the hyperbolic paraboloid $\Gamma_{\varphi\theta\alpha}$ which best fits the cloud \mathcal{N} .

2.2. Statistical fit measurement

Next we will calculate to what extent that surface statistically explains the cloud \mathcal{N} . For these calculations, we will use correlation ratio η^2 , see Eq. [9]:

$$\eta^2 = 1 - \frac{\sum_{i=1}^{i=n} (z_i - f(x_i, y_i))^2}{\sum_{i=1}^{i=n} (z_i - \bar{Y})^2} \quad [9]$$

where $\bar{Y} = \frac{1}{n} \sum_{i=1}^{i=n} z_i$, and where $(x_i, y_i, f(x_i, y_i))_{\varphi\theta\alpha}$ are the coordinates of a point of the corresponding regression surface $\Gamma_{\varphi\theta\alpha}$; that is [10]:

$$f(x_i, y_i) = \frac{-1}{J} (Bx_i^2 + Cy_i^2 + Hx_i + Iy_i + 1) \quad [10]$$

Adjusted coefficient η_{adj}^2 is given by Eq. [11]:

$$\eta_{adj}^2 = 1 - \left[(1 - \eta^2) \right] \frac{n-1}{n-d_1-1} \quad [11]$$

where $d_1 = 5$ is the number of parameters of the regression surface. We know that $\eta_{adj}^2 \in [0, 1]$ in all cases, and the value

$\eta_{adj}^2 * 100 = d_{\varphi\theta\alpha}$ is the proportion in which the variable $(z_i)_{\varphi\theta\alpha}$ of cloud \mathcal{N} is statistically explained by the least-squares correlation between $(z_i)_{\varphi\theta\alpha}$ and $(x_i, y_i)_{\varphi\theta\alpha}$. In other words, this value $d_{\varphi\theta\alpha}$ indicates the percentage of the variable $(z_i)_{\varphi\theta\alpha}$ of cloud \mathcal{N} which is statistically explained by the corresponding regression surface $\Gamma_{\varphi\theta\alpha}$. Namely, $d_{\varphi\theta\alpha}$ is a statistical measurement of how well the regression paraboloid $\Gamma_{\varphi\theta\alpha}$ fits \mathcal{N} .

2.3. Best fit

Using a calculation software that we created with C++, we repeat all the above calculations for each triplet $(\varphi, \theta, \alpha) \in [0, \pi) \times [0, \pi) \times [0, \pi)$. The three amplitudes vary in a discrete manner –not in a continuous manner–, with successive increments of 0.005 radians. Therefore, we repeat the calculation $625^3 = 244140625$ times. Each triplet $(\varphi, \theta, \alpha)$ corresponds to one of the 625^3 references $\mathcal{R}_{\varphi\theta\alpha}$ which are the rotations of the initial reference \mathcal{R}' . For each rotation we obtain the surface $\Gamma_{\varphi\theta\alpha}$, which has its own statistical fit measurement $d_{\varphi\theta\alpha}$. We calculate the maximum value of the 625^3 fit measurements $d_{\varphi\theta\alpha}$. This maximum value is obtained for certain values φ_δ , θ_δ and α_δ , and we call it $\delta = d_{\varphi_\delta \theta_\delta \alpha_\delta}$.

Having determined this maximum value δ , we obtain the hyperbolic paraboloid which in reference system $\mathcal{R}_{\varphi_\delta \theta_\delta \alpha_\delta} = \{O; \bar{e}_{1\delta}, \bar{e}_{2\delta}, \bar{e}_{3\delta}\} = \{O; \bar{e}_{1\delta}, \bar{e}_{2\delta}, \bar{e}_{3\delta}\}$ is described by the equation $0 = B_\delta x^2 + C_\delta y^2 + H_\delta x + I_\delta y + J_\delta z + 1$ and which corresponds to this maximum δ . This is the hyperbolic paraboloid which statistically best fits the cloud \mathcal{N} ; we will refer to this hyperbolic paraboloid as Γ_δ , we will refer to this reference system as $\mathcal{R}_\delta = \mathcal{R}_{\varphi_\delta \theta_\delta \alpha_\delta}$, and the coordinates determined by \mathcal{R}_δ are noted as $(x, y, z)_\delta$. The results for vaults 5 and 7 are displayed graphically in Figures 6 and 7, respectively.

However, these coordinates $(x, y, z)_\delta$ of the system $\mathcal{R}_\delta = \{O; \bar{e}_{1\delta}, \bar{e}_{2\delta}, \bar{e}_{3\delta}\}$, as well as the equation $0 = B_\delta x^2 + C_\delta y^2 + H_\delta x + I_\delta y + J_\delta z + 1$, are not intrinsic parameters of Γ_δ because they depend on the initial 3D orthonormal coordinate system $\mathcal{R}' = \{O; \bar{u}_1, \bar{u}_2, \bar{u}_3\}$ of the scanning device.

The origin O of the coordinate system \mathcal{R}_δ is translated to the vertex V_δ of Γ_δ . Thus, we obtain the orthonormal coordinate system $\mathcal{R}_{V_\delta} = \{V_\delta; \bar{e}_{1\delta}, \bar{e}_{2\delta}, \bar{e}_{3\delta}\}$. In order to do this translation, it must be borne in mind that the coordinates of V_δ are [12]:

$$V_\delta = \left(-\frac{H_\delta}{2B_\delta}, -\frac{I_\delta}{2C_\delta}, \frac{(I_\delta)^2}{4C_\delta J_\delta} + \frac{(H_\delta)^2}{4B_\delta J_\delta} - \frac{1}{J_\delta} \right) \quad [12]$$

In the system $\mathcal{R}_{V_\delta} = \{V_\delta; \bar{e}_{1\delta}, \bar{e}_{2\delta}, \bar{e}_{3\delta}\}$ we have the coordinates $(\bar{x}, \bar{y}, \bar{z})_{V_\delta}$, such that $V_\delta = (0, 0, 0)_{V_\delta}$ and the equation for surface Γ_δ is either [13]:

$$\Gamma_\delta \equiv \frac{\bar{x}^2}{(\bar{a}_\delta)^2} - \frac{\bar{y}^2}{(\bar{b}_\delta)^2} = 2\bar{z} \quad \text{or} \quad \Gamma_\delta \equiv -\frac{\bar{x}^2}{(\bar{a}_\delta)^2} + \frac{\bar{y}^2}{(\bar{b}_\delta)^2} = 2\bar{z} \quad [13]$$

With regard to calculations, the reader must take into account that $(\bar{a}_\delta)^2 = \frac{J_\delta}{2B_\delta}$ and $(\bar{b}_\delta)^2 = \frac{J_\delta}{2C_\delta}$.

In the event that $\Gamma_\delta \equiv -\frac{\bar{x}^2}{(\bar{a}_\delta)^2} + \frac{\bar{y}^2}{(\bar{b}_\delta)^2} = 2\bar{z}$, we would use $\mathcal{R}_{r_\delta}^- = \{V_\delta; \bar{e}_{1\delta}, \bar{e}_{2\delta}, -\bar{e}_{3\delta}\}$ as the reference system; in this case the equation of the surface Γ_δ is $\frac{\bar{x}^2}{(\bar{a}_\delta)^2} - \frac{\bar{y}^2}{(\bar{b}_\delta)^2} = 2\bar{z}$. In the event that $(\bar{a}_\delta)^2 > (\bar{b}_\delta)^2$ we would use $\mathcal{R}_{r_\delta}^+ = \{V_\delta; \bar{e}_{2\delta}, \bar{e}_{1\delta}, \bar{e}_{3\delta}\}$ as the reference system in order to ensure that $(\bar{a}_\delta)^2 < (\bar{b}_\delta)^2$ in the equation $\Gamma_\delta \equiv \frac{\bar{x}^2}{(\bar{a}_\delta)^2} - \frac{\bar{y}^2}{(\bar{b}_\delta)^2} = 2\bar{z}$. Hereinafter, the coordinate system \mathcal{R}_{r_δ} or $\mathcal{R}_{r_\delta}^-$ or $\mathcal{R}_{r_\delta}^+$ (where the equation of surface Γ_δ is the one described above) is called system $\bar{\mathcal{R}} = \{V_\delta; \bar{v}_1, \bar{v}_2, \bar{v}_3\}$.

Nonetheless, the parameters $\bar{a}_\delta, \bar{b}_\delta$, are not intrinsic parameters of the surface Γ_δ yet, because they still depend on the initial 3D orthonormal coordinate system $\mathcal{R}' = \{O; \bar{u}_1, \bar{u}_2, \bar{u}_3\}$ of the scanning device. Therefore, we create the orthonormal coordinate system $S_{r_\delta} = \{V_\delta; \bar{u}_{1\delta}, \bar{u}_{2\delta}, \bar{u}_{3\delta}\}$ such that [14].

$$\bar{u}_{1\delta} = \bar{v}_1, \bar{u}_{2\delta} = \bar{v}_2, \bar{u}_{3\delta} = (\bar{a}_\delta)^2 \bar{v}_3 \quad [14]$$

In this system $S_{r_\delta} = \{V_\delta; \bar{u}_{1\delta}, \bar{u}_{2\delta}, \bar{u}_{3\delta}\}$, points have coordinates (x, y, z) , such that $V_\delta = (0, 0, 0)$ and the equation of the surface Γ_δ is as follows [15]:

$$\Gamma_\delta \equiv x^2 - \frac{y^2}{b^2} = 2z \quad [15]$$

The parameter $b^2 = \frac{(\bar{b}_\delta)^2}{(\bar{a}_\delta)^2} = \frac{B_\delta}{C_\delta}$ is greater than or equal to 1, and now it is an intrinsic parameter of the surface Γ_δ . Equation [15] is an intrinsic equation of Γ_δ –it is the normalized equation of this surface.

2.4. Geometric elements

In order to geometrically understand the normalized Eq. [15], the following has to be taken into account: In order to geometrically and dynamically generate any hyperbolic paraboloid H ,

we start with a director parabola p_d (on a plane σ_d , with focal point F_d , major axis x_d and straight directrix r_d) and a generating parabola p_g (on a plane σ_g , with focal point F_g , major axis x_g and straight directrix r_g). The results for vaults 5 and 7 are displayed graphically in Figures 6 and 7, respectively. Both parabolas have the same vertex V and the same major axis $x_d = x_g$, but the plane σ_d is orthogonal to the plane σ_g and the vertex V is located between both focal points $F_d - V - F_g$. We dynamically slide the generating parabola p_g on the director parabola with a continuous movement, such that the sliding of the generating parabola p_g keeps the vertex on the director parabola p_d . This sliding is parallel to plane σ_g . This movement geometrically generates the hyperbolic paraboloid H . The director parabola has the parameter k_d and the generating parabola has the parameter k_g . Parameter k_d is the distance between the focal point F_d and the straight directrix r_d , and parameter k_g is the distance between the focal point F_g and the straight directrix r_g .

Lastly, in order to understand the equation [15] it should be noted that, by normalizing the distances so that $k_d = 1$ and $k_d \leq k_g$, in the case of the hyperbolic paraboloid Γ_δ we find that $k_g = b^2$. Furthermore, owing to the aforementioned changes of reference system, the equation of surface Γ_δ reduces to Eq. [15].

However, there is another numerical parameter which is intrinsic to Γ_δ , since it is determined by the geometry of this surface. In order to understand this parameter, the following has to be taken into account: After generating a hyperbolic paraboloid H , the vertex V of the director parabola p_d and the generating parabola p_g becomes the vertex of H . The major axis $x_d = x_g$ of the parabolas is perpendicular to the plane tangent to H in V . We call this tangential plane σ_v . The intersection of σ_v and H consists of two straight lines which we call s_1 and s_2 (Figures 6 and 7). These straight lines s_1 and s_2 (both included in H , which is a ruled surface), plus the major axis $x_d = x_g$, determine the planes π_1 and π_2 , respectively. These planes π_1 and π_2 (which, as has just been said, intersect in the axis $x_d = x_g$ of the hyperbolic paraboloid H) are the so-called director planes of H , and the straight lines s_1 and s_2 are the so-called straight directrices of H .

These director planes have the following geometric trait: through every point in H there are two straight lines which lie on H and generate the ruled surface H , such that one line of that pair is parallel to a director plane and the other line is parallel to the other director plane. The angles of the dihe-

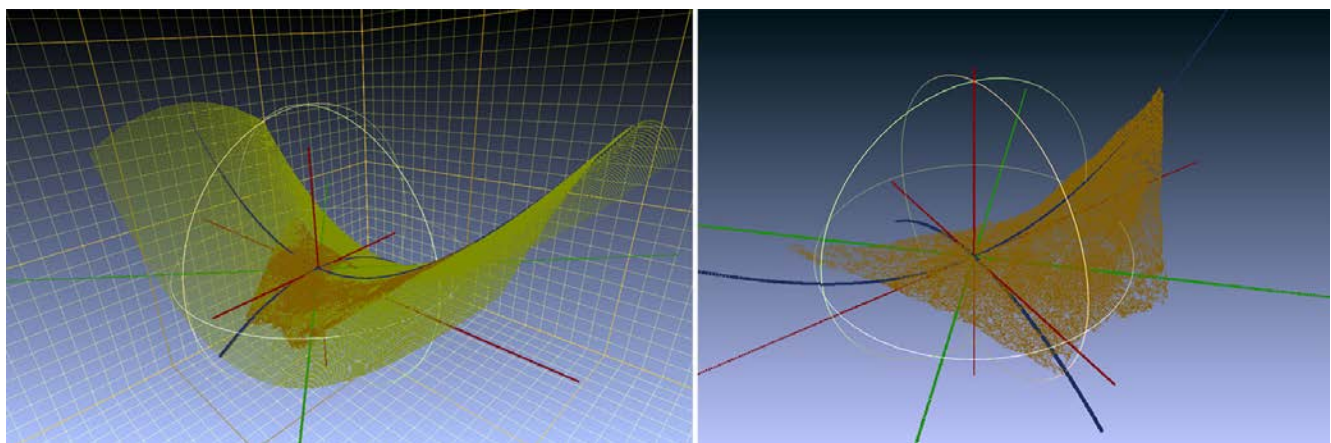


Figure 6. The cloud \mathcal{N} of vault number 5 is highlighted in orange, and its best-fitting hyperbolic paraboloid Γ_δ is highlighted in yellow. The straight directrices s_1 and s_2 are shown in green; the axes are shown in red; the director parabola p_d and the generating parabola p_g are shown in blue. [Image generated by the authors.]

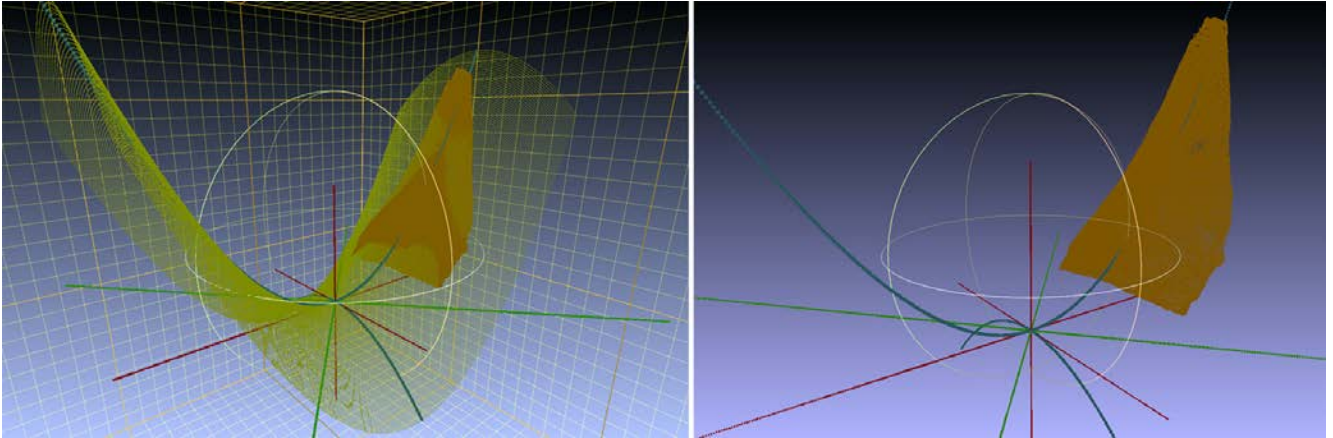


Figure 7. The cloud \mathcal{N} of vault number 7 is highlighted in orange, and its best-fitting hyperbolic paraboloid Γ_δ is highlighted in yellow. The straight directrices s_1 and s_2 are shown in green; the axes are shown in red; the director parabola p_d and the generating parabola p_g are shown in blue. [Image generated by the authors.]

dral formed by the director planes π_1 and π_2 have the same width as the angles formed by the straight directrices s_1 and s_2 . The results for vaults 5 and 7 are displayed graphically in Figures 6 and 7, respectively. If the width of the acute angles is known, then the width of the obtuse angles is also known. Hereinafter, the width of the acute angles is called α .

The numerical parameter α is intrinsic to H . In the case of the hyperbolic paraboloid Γ_δ , we have the following analytic formulas for the numerical calculation of α [16-19]:

$$m_1 = \sqrt{-4C_\delta + (I_\delta)^2 - 4B_\delta C_\delta - 4C_\delta H_\delta - 4C_\delta J_\delta \left(\frac{(I_\delta)^2}{4C_\delta J_\delta} + \frac{(H_\delta)^2}{4B_\delta J_\delta} - \frac{1}{J_\delta} \right)} \quad [16]$$

$$m_2 = \left(1 + \frac{H_\delta}{2B_\delta} \right)^2 + \left(\frac{m_1 - I_\delta}{2C_\delta} + \frac{I_\delta}{2C_\delta} \right) \left(\frac{-m_1 - I_\delta}{2C_\delta} + \frac{I_\delta}{2C_\delta} \right) \quad [17]$$

$$m_3 = \sqrt{\left(1 + \frac{H_\delta}{2B_\delta} \right)^2 + \left(\frac{m_1 - I_\delta}{2C_\delta} + \frac{I_\delta}{2C_\delta} \right)^2} \sqrt{\left(1 + \frac{H_\delta}{2B_\delta} \right)^2 + \left(\frac{-m_1 - I_\delta}{2C_\delta} + \frac{I_\delta}{2C_\delta} \right)^2} \quad [18]$$

$$\alpha = \arccos\left(\frac{m_2}{m_3}\right) \text{ if } \frac{m_2}{m_3} \geq 0, \alpha = \pi - \arccos\left(\frac{m_2}{m_3}\right) \text{ if } \frac{m_2}{m_3} < 0 \quad [19]$$

The statistical concepts used in this paper, such as the correlation ratio in [9] and the adjusted coefficient in [11], can be found in several books, for instance, in the well-known references (12, pp: 264-265; 13, pp: 584-585). The numerical concepts of the Gauss normal equations can be found, for instance, in the famous reference (14, pp: 671-675). The classification and analysis of quadratic surfaces can be found in many modern books, such as (15, pp: 559-592), and also in old books, such as the classic reference (16, pp: 200-205).

3. RESULTS

In the previous section we have provided a mathematical process to objectively determine which is the hyperbolic paraboloid Γ_δ which best fits a point cloud $\mathcal{N} = \{P_i\}_{i=1}^{i=n}$, and we have also provided an objective statistical measurement δ of that fit.

We have applied this method to the point clouds outlining the surface contours of the 19 vaults in the entrance porch to the crypt of Colònia Güell.

We have applied the above described geometric process in order to provide a normalized intrinsic analytic equation $\Gamma_\delta \equiv x^2 - \frac{y^2}{b^2} = 2z$ [15] for the best-fitting hyperbolic paraboloid Γ_δ , and we have determined its two intrinsic parameters α and b^2 .

Table 2 below shows the results for the 19 vaults of the entrance porch (α is expressed in sexagesimal degrees).

4. CONCLUSIONS

In the introduction to this paper we said that, when talking about the architectural composition and morphology of the entrance porch to the crypt of Colònia Güell, it is commonly

Table 2. Results for the 19 vaults of the entrance porch (α is expressed in sexagesimal degrees).

	δ	α	b^2
1	99.67	0.39	88270.61
2	99.86	75.30	1.68
3	99.73	0.82	19700.29
4	99.85	0.90	16377.77
5	99.71	89.40	1.02
6	99.95	60.10	2.99
7	99.76	85.08	1.19
8	97.92	15.90	51.27
9	97.64	0.21	284071.32
10	98.85	1.37	7023.60
11	97.59	0.04	8108811.54
12	99.70	0.06	3462399.46
13	99.46	0.03	11083400.45
14	99.42	0.43	71687.29
15	99.16	0.16	531535.10
16	99.58	0.54	45211.87
17	98.36	7.89	210.34
18	99.86	0.21	307243.25
19	99.16	0.01	173306546.50

claimed that all of its 19 vaults were designed in the shape of hyperbolic paraboloids. Besides, 13 of these surfaces are decorated with coloured ceramic crosses which allegedly follow the straight directrices of these hyperbolic paraboloids.

Using photogrammetrical techniques, we obtained the point cloud outlining the surface contour of a vault in the entrance porch to the crypt of Colònia Güell. In section 2 of this paper we outline the method used to find the hyperbolic paraboloid Γ_δ which best fits this point cloud $\mathcal{N} = \{P_i\}_{i=1}^{i=n}$. Besides, we have developed a fit measurement model and found a measurement δ of how well the hyperbolic paraboloid Γ_δ fits the cloud \mathcal{N} . Also, we have laid down the necessary calculations to find the intrinsic normalized equation and the intrinsic geometric parameters a and b^2 of the hyperbolic paraboloid Γ_δ .

After carrying out these calculations, we present the intrinsic normalized equations of the 19 hyperbolic paraboloids Γ_δ which best fit the 19 vaults of the porch (see Section 3 Results). We also provide the corresponding statistical fit measurement δ of each hyperbolic paraboloid Γ_δ for each vault; and in Table 2 we display the geometric parameters a and b^2 which are intrinsic to each of the 19 hyperbolic paraboloids Γ_δ .

As a consequence of all this geometric calculation process, we conclude that 1) there is insufficient statistical evidence that vaults number 8, 9, 10, 11 and 17 were designed based on hyperbolic paraboloids (since their corresponding fit measurements δ are below 99%); and 2) there is sufficient statistical evidence (fit measurement above 99%) that the remaining fourteen vaults were designed based on hyperbolic paraboloids.

The above paragraph has the following meaning: Even if the architect had wanted to create paraboloids, the fact is that none of the surfaces generated by the 19 fragments of vaults actually are paraboloids. This is so for several reasons: building errors, materials deformations, mechanical settlements, etc. Nevertheless, maybe some of them were designed in the shape of hyperbolic paraboloids. In other words: the vault may have been built using a centering made up of straight beams which are parallel to a given director plane and rest on another straight beam (i.e., the definition of a hyperbolic paraboloid using its generatrices). In this case, we say that the vault *was designed in the shape* of a hyperbolic paraboloid. But it is also possible that the vault was not built in that way. Namely: perhaps the vault was not built using a centering as described above. In this case, we say that the vault *was not designed in the shape* of a hyperbolic paraboloid. We do not know how each of these vaults was built, so we do not know if each vault was or wasn't designed in the shape of a hyperbolic paraboloid. Therefore, we only say whether we have or we don't have enough statistical evidence of that.

With regard to the decorative crosses that are present in 13 of the 19 vaults, we find that they do not follow the straight directrices of the hyperbolic paraboloids generated by these vaults. As an example, we show the location of the cross and the straight directrices for vault number 5 (Figure 8).

It is clear that our working method –a mixture of statistics, geometry and numerical calculation– was never in the mind of Gaudí. However, it is not our intention to present a historical topic. Using the mathematical tools available to us, we intend to show the readers another point of view for studying this historical heritage.

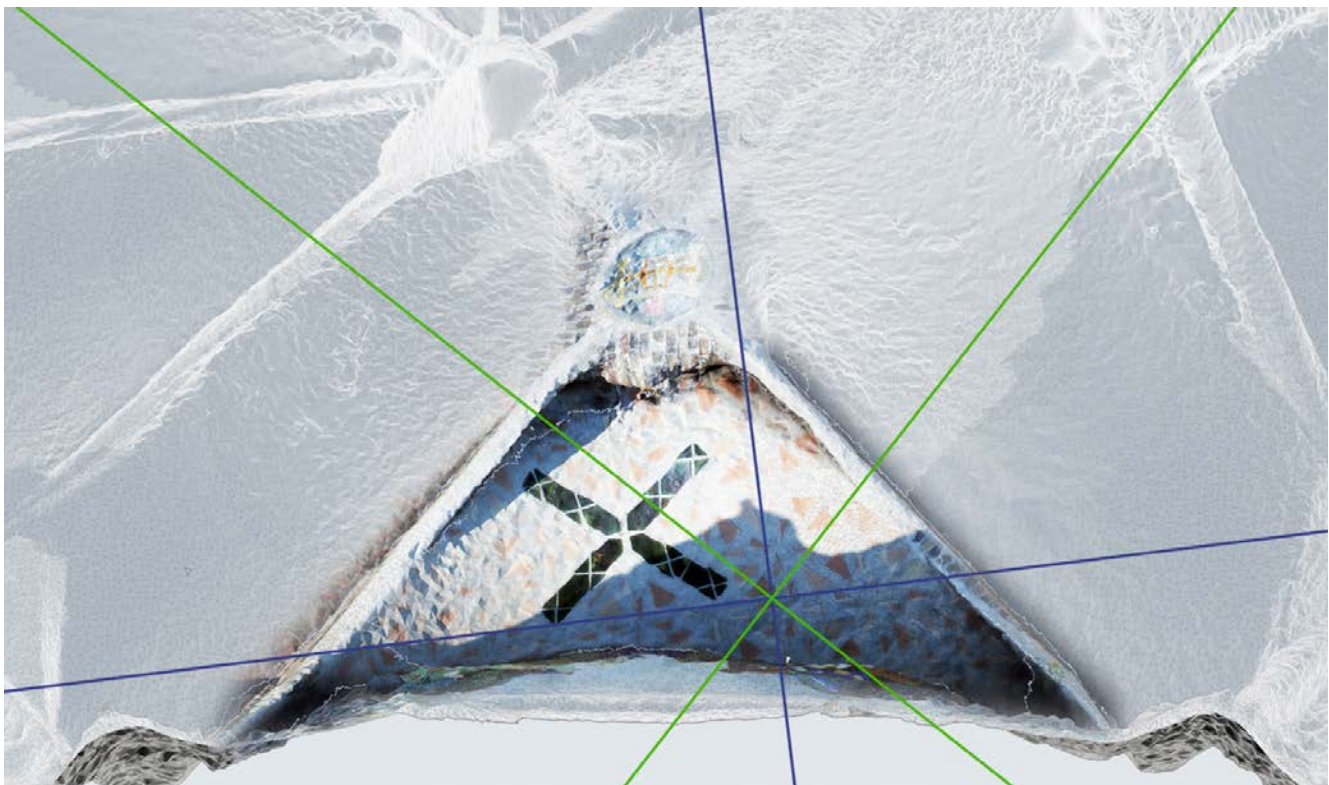


Figure 8. The ceramic cross of vault number 5 and, in green color, the straight directrices of the best-fitting hyperbolic paraboloid Γ_δ . [Image generated by the authors.]

REFERENCES

- (1) Girant Miracle, D. et al. (2002). *Gaudí, búsqueda de la forma: espacio, geometría, estructura y construcción*, Barcelona: Lunwerg.
- (2) Puig-Boada, I. (1976). *L'església de la Colònia de Güell*, Barcelona: Lumen.
- (3) González, J. L. (2000, 26 de octubre). Configuración constructiva y comportamiento mecánico de las bóvedas tabicadas en la construcción catalana del siglo XIX. *Actas del III Congreso Nacional de Historia de la Construcción* (pp. 431-436). Sevilla: Instituto Juan de Herrera.
- (4) Truñó, Á. (2004). *Construcción de bóvedas tabicadas*. Madrid: Instituto Juan de Herrera y Escuela Técnica Superior de Arquitectura de Madrid.
- (5) Bassegoda, B. (1997). *La bóveda Catalana*. Barcelona: Edición Éntasis.
- (6) González, J. L. (1999). *La bóveda tabicada. Su historia. Su futuro. Tratado de rehabilitación. Vol.1: Teoría e historia de la restauración*. Madrid: Munilla-Lería.
- (7) González, J. L. (2000, 26 de octubre). La configuración constructiva de las bóvedas "convexas" de la Iglesia de la Colonia Güell, obra de Antoni Gaudí. *Actas del III Congreso Nacional de Historia de la Construcción* (pp.437-441). Sevilla: Instituto Juan de Herrera.
- (8) Cardellach, F. (1949). Explicació de Gaudí sobre les voltes de paraboloides, i estructura arborífera. *El Propagador* 14.
- (9) Padró-Margó, J. (2003). La restauració de l'església de Gaudí de la Colònia Güell. *Materials del Baix Llobregat* 9: 77-84.
- (10) Po-Hung, L. Chin-Wei, C. (2015). An exploratory study of the geometrical elements in Gaudí's Architecture. *International Journal of arts and sciences* 8 (3): 51-58.
- (11) Huerta, S. (2006). Structural design in the work of Gaudí. *Architectural Science Review* 49 (4): 324-339, doi: <https://doi.org/10.3763/asre.2006.4943>.
- (12) Rao, C. R. (1973). *Linear Statistical Inference and its Applications, Second Edition*, p. 264-265. New York: John Wiley.
- (13) Berenson, L. M. Levine, M. D. Krehbiel, C. T. (2012). *Basic Business Statistics: concepts and applications, Twelfth Edition*, p. 584-585. New York: Prentice Hall.
- (14) William H. P. et al. (1992). *Numerical Recipes in C: The Art of Scientific Computing, Second Edition*, p. 671-675. New York: Cambridge University Press.
- (15) Hernández, E. (1994). Álgebra y Geometría, Segunda Edición, p. 559-592. Wilmington: AddisonWesley Iberoamericana.
- (16) Wilson, A.W. Tracey, J. I. (1925). *Analytic Geometry, Revised Edition*, p. 200-205. New York: D.C. Heath and Company.